

Graphical Abstract

A multi-task deep learning approach for lane-level pavement performance prediction with segment-level data

Bo Wang, Wenbo Zhang, Yunpeng Li

Highlights

A multi-task deep learning approach for lane-level pavement performance prediction with segment-level data

Bo Wang, Wenbo Zhang, Yunpeng Li

- A multi-task deep learning approach is proposed for lane-level pavement performance prediction.
- The unified prediction framework can effectively address inherent correlation and differences across lanes.
- Pavement performance indicator time series is processed using shared LSTM and task-specific head and get a initial predictions.
- Auxiliary pavement features is concatenated with initial predictions to adjust the predictions and get the final predictions.
- The model is validated on one-way 2-lane, 3-lane, and 4-lane scenarios, all lower than 10% in terms of mean absolute percentage error.

A multi-task deep learning approach for lane-level pavement performance prediction with segment-level data

Bo Wang^a, Wenbo Zhang^{a,*}, Yunpeng Li^a

^a*School of Transportation, Southeast University, Nanjing, 210000, Jiangsu, China*

Abstract

The elaborate pavement performance prediction is an important premise of implementing preventive maintenance. Our survey reveals that in practice, the pavement performance is usually measured at segment-level, where a unique performance value is obtained for all lanes within one segment of 1km length. It still lacks more elaborate performance analysis at lane-level due to costly data collection and difficulty in prediction modeling. Therefore, this study developed a multi-task deep learning approach to predict the lane-level pavement performance with a large amount of historical segment-level performance measurement data. The unified prediction framework can effectively address inherent correlation and differences across lanes. In specific, the prediction framework firstly employed a Long Short-Term Memory (LSTM) layer to capture the segment-level pavement deterioration pattern. Then multiple task-specific LSTM layers were designed based on number of lanes to capture lane-level differences in pavement performance. Finally, we concatenated multiple task-specific LSTM outputs with auxiliary features for further training and obtained the lane-level predictions after fully connected layer. The aforementioned prediction framework was validated with a real case in China. It revealed a better model performance regardless of one-way 2-lane, 3-lane, and 4-lane scenarios, all lower than 10% in terms of mean absolute percentage error. The proposed prediction framework also outperforms other ensemble learning and shallow machine learning methods in almost every lane.

*Corresponding author

Email address: wenbozhang@seu.edu.cn (Wenbo Zhang)

Keywords: Lane-level Pavement Performance, Pavement Performance Prediction, Multi-task Learning, Long Short-Term Memory

1. Introduction

The most widely used pavement performance measurements include pavement condition index (PCI), pavement quality index (PQI), and riding quality index (RQI). These measurements in a lane with shorter length can assist in identifying small but severely damaged road sections that are detrimental to traffic. The performance measurement prediction can further provide refined performance trends in future years for each lane. Utilizing the predicted lane-level performance values can further execute the preventive maintenance in a precisely and cost-effective way. Thus, lane-level performance predictions are significantly more useful for pavement maintenance than segment-level ones that merely provide one rough value for all lanes in a segment of 1 km. However, it is impossible of collecting huge amount of lane-level data in reality and directly predicting the performance in next few years. To address such difficulty, this study is dedicated to developing a lane-level pavement performance prediction framework with a large amount of segment-level data.

The different deterioration patterns across lanes are obviously one challenge for developing such unified lane-level prediction framework effective for all lanes. As shown in Figure 1, the difference in performance values across different lanes can range from -60 to 60. The prediction modeling should learn such variations in one unified modeling framework. On the other hand, due to the limited lane-level data but large amount of segment-level data, the data-driven deep learning can be more easier to capture the common deterioration pattern shared by all lanes. It is possible of incorporating the segment-level deterioration pattern into the lane-level prediction to further enhance prediction accuracy.

The state-of-the-art studies have already proposed models for segment-level pavement performance prediction while existing fewer lane-level prediction modeling frameworks. Few of them also developed machine learning-based methods, such as artificial neural networks^[1] and random forest^[2], which yield good prediction accuracy. However, these models are not discussed at lane-level and cannot capture the differences across lanes.

To address the difficulties during lane-level performance prediction, we propose a multi-task deep learning approach for lane-level pavement performance prediction based on segment-level data to deal with those challenges.

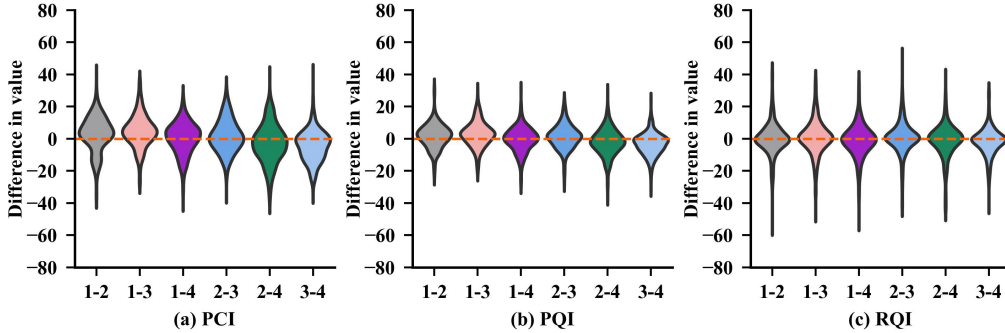


Figure 1: The distribution of the difference in PCI, PQI, and RQI between two lanes. Note: The ‘1-2’ label on x-axis means the performance difference between lane 1 and lane 2. Lane 1 is the innermost lane. This is applicable to other labels.

The model employs an LSTM-based shared layer to capture the common and representative changing pattern information from pavement performance time series. Based on the shared information, the task-specific heads are used to extract the details and changes related to a specific lane and generate predictions for the lane. Subsequently, the predictions are horizontally concatenated with auxiliary features, and the features distinguish roads with different decay patterns. At last, the task-specific output layer will handle the concatenation results to get the final lane-level predictions. To verify the proposed model, the real case was employed to check prediction accuracy of PCI, PQI, and RQI on three scenarios including one-way 2-lane, 3-lane, and 4-lane roads.

The remainder of this paper is organized as follows: In section 2, we summarize the related work on pavement performance prediction. In section 3, we present the structure of the proposed model. Then, we validate the model through comparative and ablation experiments based on a dataset collected on our own in section 4. Finally, we present our conclusions and offer guidelines for future work.

2. RELATED WORK

Pavement performance prediction models can be categorized into two types: Non-data-driven and data-driving models. The former rely on specific mathematical equations or physical principles. Still, the latter primarily

relies on a large amount of data input rather than solely on theoretical assumptions or prior knowledge.

2.1. Non-data-driven models

Non-data-driven models predict pavement performance based on deterministic principles and equations, like empirical formula models and mechanical models. They can also take into account random factors in pavement performance deterioration and use probability and statistics methods, such as Markov models and Monte Carlo simulations, to describe the possible distribution or changing trend of pavement performance. Wu compared the effectiveness of pavement performance prediction based on S-shaped model, polynomial model, and exponential model. And the S-shaped model demonstrates the best predictive performance^[3]. Cao selected service life and cumulative number of axle loads as independent variables and applied cosine deterioration equation to predict PCI and rutting depth index of roads with excellent pavement performance^[4]. Sidess combining empirical-mechanistic approach and regressive empirical approach to predicting the international roughness index^[5]. Wang calibrated parameters of the rutting prediction model for semi-rigid base asphalt pavement in MEPDG based on real data From Xi'an, China^[6]. Dong predicted asphalt pavement performance utilizing Markov models based on insufficient inspection data^[7]. Wang put forward a Grey–Markov combination model to predict PCI^[8]. Since pavement deterioration rate may not be constant, Abaza developed a non-homogeneous Markov chain, which uses different transition matrix to predict future pavement performance for every time step^[9]. Besides, Wasiq proposed a hybrid approach combining both homogeneous and non-homogeneous Markov Chain to predict the PCI^[10].

Non-data-driven models are not suitable for considering the complex relationships between various factors and the coupled effects of some factors on pavement performance degradation.

2.2. Data-driven models

data-driven Models do not rely on specific mathematical equations or physical principles, but rather learn patterns in the data through algorithms and are used for the prediction of pavement performance. Wang developed a hybrid grey relation analysis and support vector machine regression model to predict pavement performance^[11]. Xiao combined particle swarm optimization algorithm and back propagation neural network to predict asphalt

pavement performance^[12]. Tao proposed a differential evolution particle swarm optimization back propagation neural network to predict PCI^[13]. Abdulmtalab investigated the combined effect of pavement distress on flexible pavement performance in two climate regions (wet freeze and wet no freeze) separated using multiple linear regression and artificial neural network^[14]. Cai proposed a Causal-Temporal Graph Convolution Network, combining the Graph Convolution Networks) and LSTMs to capture causal features and temporal features simultaneously, to predict pavement performance^[15]. Bukharin proposed a two-stage model combining LSTM and artificial neural network (ANN). The LSTM is used to learn the pavement deterioration pattern based on sequential data and ANN further learns the factors influencing deterioration to adjust the final predictions^[16]. Guo proposed a weighted multi-output neural network to predict IRI, faulting, longitudinal crack and transverse crack simultaneously^[17].

Data-driven models are more suitable for performance prediction of a large number of road segments, and they can capture different decay patterns of the road segments as well as the relationship between segments' decay and influencing factors. Also it is suitable for extracting the similarity and difference of lanes' decay patterns.

3. METHODS

3.1. Problem definition

This paper is dedicated to proposing a lane-level pavement performance prediction model. The prediction is based on segment-level pavement inspection data, and static factors influencing pavement deterioration.

$$\hat{y}_{t+1,N} = f(y_{t-k:t}, x_{t-k:t}, S) \quad (1)$$

where:

$\hat{y}_{t+1,N}$ is the predicted performance value of each lane,

N is the number of lanes,

$y_{t-k:t}$ is the predictive indicator's time series from time step $t - k$ to time step t , like PCI, PQI and RQI,

$x_{t-k:t}$ are the covariates' time series from time step $t - k$ to time step t ,

S is the static covariates in the observational process that are invariant.

For instance, pavement material,

$f(\cdot)$ is the relationship between the predictive indicator and covariates.

3.2. Model overview

In this section, we focus on introducing the structure of the proposed multi-task deep learning model (MTL), as shown in Figure 2. The LSTM-based shared layer, module (a) in Figure 2, will extract general decay patterns of different lanes from the pavement performance time series. Then, the output of the layer will be sent to module (b); the module consists of an LSTM and a fully connected layer (FC layer in Figure 2). The LSTM will predict based on the output, and the fully connected layer will encode the predictions. In module (c), the encoded predictions will be horizontally concatenated with auxiliary features. The concatenation result will be sent to each fully connected layer followed. The fully connected layer will adjust the prediction using auxiliary features and then get the final lane-level prediction results.

3.2.1. LSTM-based shared layer

The LSTM-based shared layer is initially used to handle the pavement performance time series. It is responsible for discovering and extracting common decay patterns of different lanes. LSTM is a type of recurrent neural network architecture designed to handle the vanishing and exploding gradient problems often encountered in traditional recurrent neural networks when dealing with long data sequences. LSTM units have a more complex internal structure than standard recurrent neural network cells. They consist of three main gates: the input gate, the forget gate, and the output gate. The input gate decides how much new information to let into the cell state, the forget gate determines which parts of the previous cell state to discard, and the output gate controls how much of the cell state is output as the hidden state. This gated mechanism allows LSTMs to selectively remember or forget information over long intervals, making them well-suited for time series prediction tasks.

(1) Forget gate:

The forget gate controls what information is removed from the memory cell. Two inputs x_t (input at the particular time t) and h_{t-1} (previous cell output) are fed to the gate and multiplied with weight matrices followed by the addition of bias. The resultant is passed through an activation function which gives a binary output. If for a particular cell state, the output is 0, the piece of information is forgotten and for output 1, the information is retained for future use.

$$f_t = \sigma(W_f[h_{t-1}, x_t] + b_f) \quad (2)$$

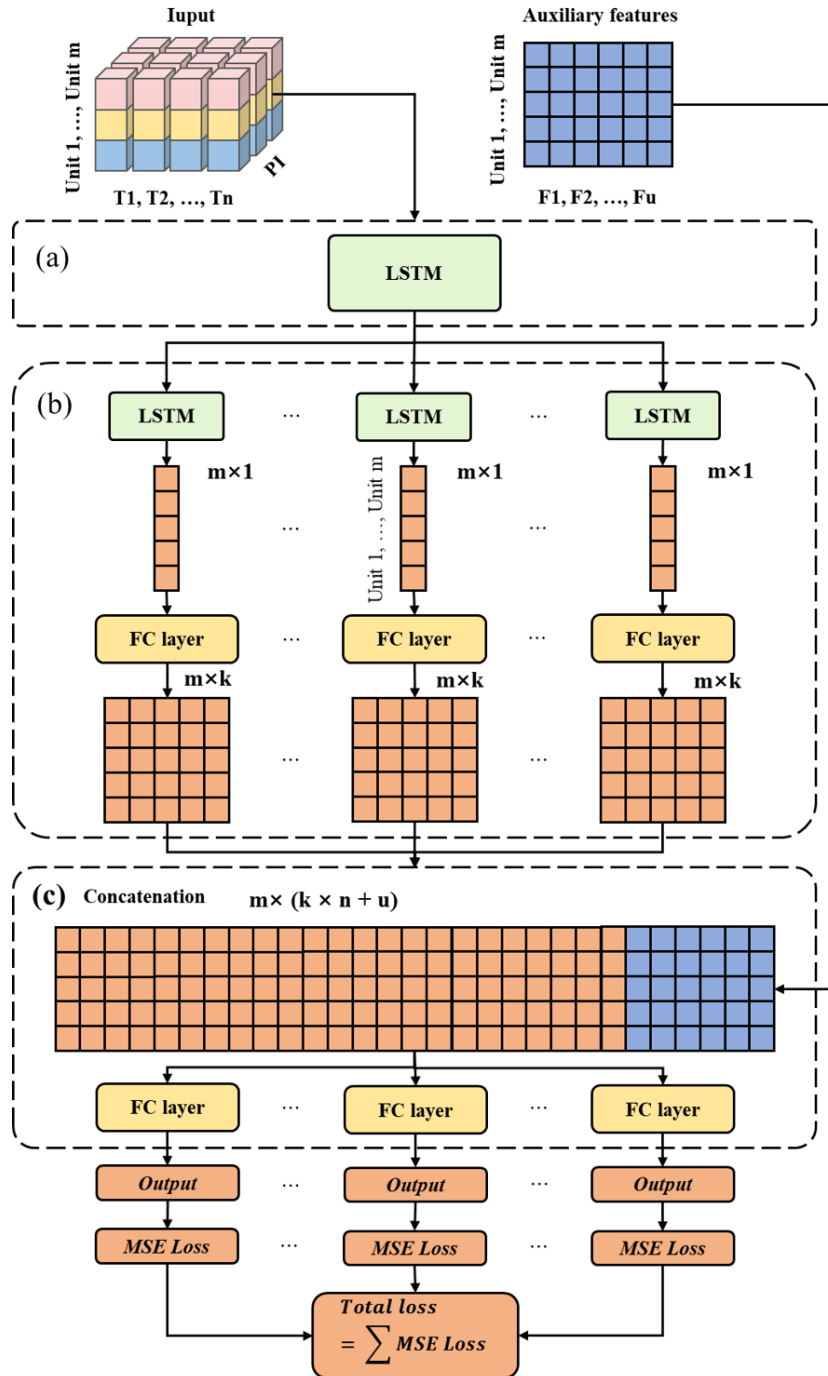


Figure 2: The overall lane-level prediction modeling structure

(2) Input gate:

The input gate controls what information is added to the memory cell. First, the information is regulated using the sigmoid function and filter the values to be remembered similar to the forget gate using inputs h_{t-1} and x_t . Then, a vector is created using tanh function that gives an output from -1 to +1, which contains all the possible values from h_{t-1} and x_t . At last, the values of the vector and the regulated values are multiplied to obtain the useful information. The equation for the input gate is:

$$i_t = \sigma(W_i[h_{t-1}, x_t] + b_i) \quad (3)$$

$$\tilde{c}_t = \tanh(W_c[h_{t-1}, x_t] + b_c) \quad (4)$$

We multiply the previous state by f_t , disregarding the information we had previously chosen to ignore. Next, we include $i_t * C_t$. This represents the updated candidate values, adjusted for the amount that we chose to update each state value.

$$c_t = f_t \odot c_{t-1} + i_t \odot \tilde{c}_t \quad (5)$$

(3) Output gate:

The output gate controls what information is output from the memory cell. First, a vector is generated by applying tanh function on the cell. Then, the information is regulated using the sigmoid function and filter by the values to be remembered using inputs h_{t-1} and x_t . At last, the values of the vector and the regulated values are multiplied to be sent as an output and input to the next cell. The equation for the output gate is:

$$o_t = \sigma(W_o[h_{t-1}, x_t] + b_o) \quad (6)$$

For each time step t , the hidden state h_t will be updated by the input of vector x_t , previous hidden cell state h_{t-1} and previous cell state c_{t-1} . The vector formulas of pass forward along timesteps can be written as:

$$h_t = o_t \odot \tanh(c_t) \quad (7)$$

Where W_* and b_* denotes the weight matrix and bias of the corresponding gates respectively, $\sigma()$ is the sigmoid activation function, \tanh is the hyperbolic tangent activation function, \odot is the Hadamard product, which denotes an element-wise product, and c_t is designed to accumulate the short memory.

3.2.2. Multiple task-specific heads

The multiple task-specific heads, module (b) in Figure 2, is designed to generate predictions for each lane, allowing the model to learn unique pavement performance decay patterns. Each head comprises an LSTM unit and a fully connected layer that employs the Leaky Rectified Linear Unit (LeakyReLU) activation function. The LSTM component is instrumental in predicting pavement performance by analyzing the time series data derived from the LSTM-based shared layer. The fully connected layer that follows serves a dual purpose: it maps the LSTM’s predictions to a tailored range or space, and enhances the model’s capacity to distill and articulate a rich tapestry of features.

$$y_k = g \left(\sum_{j=1}^J w_{jk} x_j + b_k \right) \quad (8)$$

Where g is activation function, J is the number of neurons, w_{jk} is the weight from neuron j of the previous layer to neuron k , x_j is the input from neuron j , and b_k is the bias for neuron k .

In deep neural networks, the gradients may gradually decrease during back propagation, making the model difficult to train. The LeakyReLU activation function has a non-zero gradient for negative inputs, which helps the gradients propagate more effectively in the network, thereby accelerating the training and convergence of the model. The mathematical expression for the LeakyReLU is:

$$F(x) = \begin{cases} x, & \text{if } x \geq 0 \\ \alpha x, & \text{if } x < 0 \end{cases} \quad (9)$$

Where α is a small constant, often chosen between 0.01 and 0.1.

3.2.3. Multiple task-specific output layers

Multiple task-specific output layers, module (c) in figure 2, are used to transform the concatenation result, a two-dimensional tensor consisting of initial prediction and auxiliary features of lanes, into final lane-level predictions. Each task-specific output layer is responsible for a specific lane.

$$\hat{\mathbf{Y}}_{\mathbf{n}} = \mathbf{X} \times \mathbf{W}_{\mathbf{n}} \quad (10)$$

$$\hat{\mathbf{Y}}_{\mathbf{n}} = [\hat{\mathbf{y}}_{n1}, \hat{\mathbf{y}}_{n2}, \dots, \hat{\mathbf{y}}_{n\rho}] \quad (11)$$

Where $\widehat{\mathbf{Y}}_n$ is the final predictions of lane n , n is the lane number, \mathbf{X} is the concatenation result, \mathbf{W}_n is the weight matrix of task-specific output layer for lane n , and ρ is the number of prediction units.

3.2.4. Total loss calculation

In a multi-task learning-based model, the loss function feedback mechanism balances the training of various tasks, ensuring that each task benefits from improvements. In our model, the loss function is the aggregate of the losses from each pavement prediction task. Once the total loss is calculated, parameter updates are executed through the gradients derived from the loss function.

$$L_{Total} = L_1 + L_2 + \dots + L_N \quad (12)$$

$$L_n = \frac{1}{\rho} \sum_{i=1}^{\rho} (y_i - \hat{y}_i)^2 \quad (13)$$

Where L_{Total} is the total loss of model training, N is the number of lanes, L_n is the MSE loss for the pavement prediction of lane n , y_i is the actual value of prediction unit i , and \hat{y}_i is the predicted value of prediction unit i .

4. REULSTS

4.1. Dataset and preprocessing

The pavement inspection dataset from Zhengzhou, Jiaozuo, and Luoyang in Henan Province, China, covering 2020 to 2023, was used for model verification. The data from 2020 to 2022 is segment-level and recorded in units of 1000m (around 0.6 mile); the data from 2023 is lane-level and recorded in units of 100m (around 0.06 mile). The dataset records road names, the direction of travel (upstream and downstream), milepost numbers, pavement performance indicators (such as PCI, PQI, and RQI), pavement surface material, etc. A comprehensive introduction of features is delineated in TABLE 1. To verify the general effectiveness of the model in different task quantities and indicator predictions, we establish three distinct datasets, 2-lane, 3-lane, and 4-lane, each dataset consisting of the road with a corresponding number of lanes. Each dataset will be used to predict PCI, PQI, and RQI.

All available datasets are collected from 2020 to 2023 and matched based on road name, direction, and mileposts. Consequently, time series can be formed for three pavement performance indicators, including PCI, PQI, and

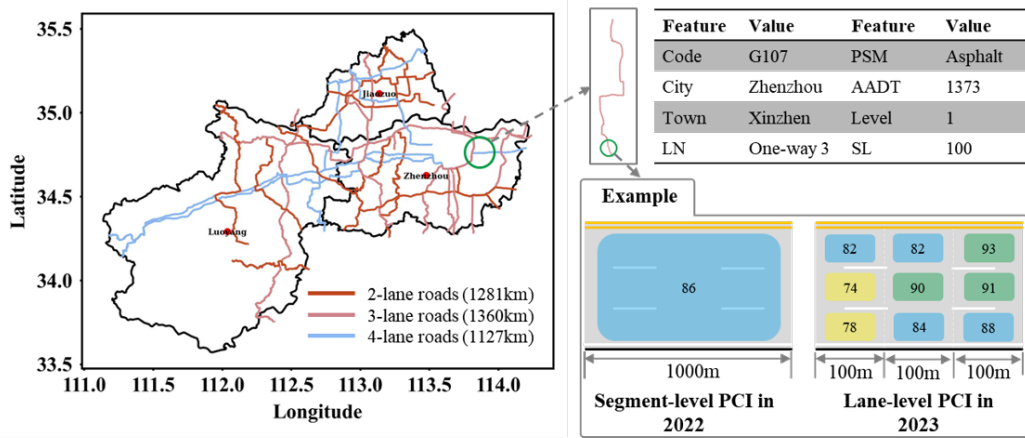


Figure 3: The description of study case in Henan province, China

Table 1

The features collected in the study case

No.	Feature name	Description	Type	Ranges
1	PCI	Pavement Condition Index	Continuous	From 0 to 100
2	PQI	Pavement Quality Index	Continuous	From 0 to 100
3	RQI	Riding Quality Index	Continuous	From 0 to 100
4	Code	Road name	Discrete	G107, S323, etc.
5	Dir.	Upstream or downstream direction of road	Discrete	Upstream, downstream
6	Level	The classification of road	Discrete	From 1 to 4
7	City	The city where the road segment is located	Discrete	Zhennzhou, Luoyang, Jiaozuo city
8	Town	The town where the road segment is located	Discrete	Jinshui district, Erqi district, etc.
9	SL	Speed limit of the road	Continuous	From 60 to 120
10	AADT	Average Annual Daily Traffic	Continuous	From 50 to 3000
11	PSM	pavement surface material	Discrete	Asphalt, concrete
12	LN	Lane number, The innermost is lane 1	Discrete	From 1 to 4

Note: Discrete features will be encoded using one-hot encoding.

Table 2

The data samples in three road scenarios

Dataset	PCI	PQI	RQI
2-lane dataset	524	536	516
3-lane dataset	705	792	678
4-lane dataset	716	812	848

RQI. Only the time series that demonstrate a year-by-year degradation in pavement performance are retained. Because when pavement is not maintained, its performance is expected to continue declining. We do not take into account performance predictions in the presence of road maintenance disturbances. The final number of time series is presented in TABLE 2. Each dataset, including time series for PCI, PQI, and RQI and auxiliary features, will be partitioned into training and testing subsets with a ratio of 70:30. Features excluding PCI, PQI, and RQI in each training set will undergo independent Z-score normalization. And the same features in the corresponding test set will then be standardized using the mean and variance derived from their respective training sets. This approach ensures that the model training phase does not inadvertently incorporate test set information and guarantees that the scale and distribution of the test data match those of the training data. This alignment facilitates a fair and accurate assessment of the model’s performance.

4.2. Evaluation metrics

Mean absolute percentage error(MAPE) is employed to assess the performance of our model. MAPE reflects the average relative deviation of the predicted values from the actual values and is not influenced by the magnitude of the data. The smaller their values, the better the performance of the model. The calculation formula is as follows:

$$MAPE_n = \frac{1}{m} \sum_{j=1}^m \left| \frac{y_{nj} - \hat{y}_{nj}}{y_{nj}} \right| \times 100\% \quad (14)$$

$$MAPE_{Total} = \frac{1}{N} \sum_{n=1}^N MAPE_n \quad (15)$$

Where n is the lane number, $MAPE_n$ is the MAPE of lane n , m is the number of prediction units in lane n , \hat{y}_{nj} is the j^{th} unit’s predicted value of

Table 3
Output shape of typical model components

No.	Layer	Output shape
1	Input	$m \times 3 \times 1$
2	LSTM based shared layer	$m \times 3 \times 1$
3	LSTM in task-specific head	$m \times 1$
4	Fully connected layer in task-specific head	$m \times 32$
5	Task-specific output layer	$m \times 1$

Note: m is the number of prediction units.

lane n , y_{nj} is the j^{th} unit’s actual value of lane n , $MAPE_{Total}$ is the MAPE of all lanes, and N is the number of lanes.

4.3. Model setting

The model parameters can be set as follows. The LSTM-based shared layer, module(a) in Figure 2, includes two layers with a hidden layer of dimension 128. In the multiple task-specific heads, module(b) in Figure 2, the LSTM contains two layers with a hidden layer of dimension 64, and a fully connected layer has two layers with a hidden layer of dimension 64 and an output layer of dimension 32. The activation function employed in the fully connected layers is the LeakyReLU. The number of task-specific heads is variable, aligning with the number of lanes, and ranges from two to four. The fully connected layer in the multiple task-specific output layers is of size 32 and output dimension 1. The hyperparameters that underpin our model include, but are not limited to, the learning rate, batch size, and the number of training epochs. In our experiment, the learning rate is 0.001, the batch size is 32, and the model is subjected to 200 training epochs. The output of each layer is shown in Table 3.

4.4. Model performance

The following models are selected to compare the performance of our model:

- (1) LSTM. It can effectively handle the long-term dependencies in sequential data.
- (2) GRU. Gated Recurrent Unit. It is similar to LSTM, which also introduces a gating mechanism to control the flow of information. Compared

with LSTM, it has a simpler structure, fewer parameters, and higher computational efficiency.

(3) XGBoost Regressor. eXtreme Gradient Boosting Regressor. It is a robust gradient-boosting decision tree algorithm. When making predictions, each historical value of the performance indicators is added as a feature.

(4) RF. Random Forest is an ensemble learning algorithm that builds multiple decision trees and combines their results to make the final prediction. When making predictions, each historical value of the performance indicators is added as a feature.

Two distinct experimental configurations were established, referred to as the 'lane-specific model' and the 'mix model', respectively, based on the four previously mentioned models. The lane-specific model will train a dedicated model for each lane. For instance, this strategy culminates four models within the context of a 4-lane road dataset. So, the training process of each model is not influenced by the decay patterns of other lanes. The mix model will add lane number as a feature, which is used to distinguish the decay patterns of different lanes. The model enables the concurrent generation of all lanes' predictive outputs.

The proposed model and comparative models were deployed to predict lane-level PCI, PQI, and RQI using a 2-lane, 3-lane, and 4-lane dataset. Our model demonstrates superior performance when evaluated under the MAPE metric across all three datasets and for each performance indicator: PCI, PQI, and RQI. This out-performance underscores the efficacy of our model in delivering more precise lane-level predictions. The detailed MAPE results are presented in Table 4.

Table 4
The MAPE of proposed model and benchmark models

configurations	model	2-lane dataset			3-lane dataset			4-lane dataset		
		PCI	PQI	RQI	PCI	PQI	RQI	PCI	PQI	RQI
Lane specific model	LSTM	12.554	15.133	10.543	6.743	8.221	7.862	8.382	7.600	7.602
	GRU	12.239	14.639	9.790	6.623	9.577	7.970	8.311	7.319	5.819
	XGBoost	11.977	14.202	9.985	6.199	8.711	7.063	9.073	7.605	5.440
	RF	11.707	13.973	10.057	5.946	8.419	6.698	9.952	7.076	5.693
Mix model	LSTM	13.525	12.495	10.520	6.357	8.017	6.262	8.685	7.514	5.704
	GRU	12.685	11.979	10.484	6.104	7.740	6.217	10.389	6.867	5.741
	XGBoost	11.661	11.731	10.612	5.880	7.771	6.310	10.169	6.765	6.029
	RF	11.327	11.458	10.276	5.866	7.468	5.849	10.499	6.580	5.242
MTL model	Ours	10.799	10.837	9.291	5.273	6.980	5.195	5.752	5.739	3.317

(1) Our model exhibited the most optimal performance on the 4-lane dataset, trailed by the 3-lane dataset, while the 2-lane dataset manifested the poorest performance. The MAPE was 4.936%, 5.816%, and 10.309% respectively. This phenomenon is associated with the quantity of prediction units and tasks. The greater the number of units, the more information the model acquires. Furthermore, a greater number of lanes is more conducive to enhancing the shared information.

(2) Compared with other models, our model has accomplished an average absolute maximum reduction in MAPE of 3.092%, 2.699%, and 2.774% for the 4-lane, 3-lane, and 2-lane datasets, respectively. Correspondingly, the average absolute minimum reduction in MAPE is 1.480%, 0.556%, and 0.560% for the datasets mentioned above in sequence. The outcomes manifest the effectiveness of our model in leveraging related tasks to enhance the overall forecasting accuracy in pavement performance analysis.

(3) Our model attains an average MAPE of 7.852%, 7.275%, and 5.934%, respectively, for predicting PQI, PCI, and RQI. Furthermore, as depicted in Figure 1, the dataset exhibits the maximum average PQI difference of 2.834 between different lanes, succeeded by PCI with a difference of 1.950 and RQI with a difference of 0.946. The MAPE demonstrates a specific positive correlation with the performance disparity between lanes. The positive correlation indicates that the similarity between lanes and the resemblance between tasks can mitigate the model’s prediction error.

(4) Figure 4 demonstrates lane-level MAPE results using our model. Moreover, as the number of lanes escalates, the difference in MAPE among lanes narrows. Additionally, the MAPE of lane 1 and lane 2 generally shows a downward trend because the information of the newly added prediction tasks will improve the accuracy of the existing performance prediction tasks.

(5) FIGURE 5, 6, and 7 show lane-level MAPE based on 2-lane, 3-lane, and 4-lane datasets. In most cases, the MAPE of each lane is the lowest using our model compared with the lane-specific and mix models. In the 2-lane dataset, there are 3 times, accounting for 50%, that the lane-level MAPE is not the lowest. And all are from lane 2. But in 3-lane and 4-lane datasets, the numbers that the lane-level MAPE is not the lowest are 2 and 4, only accounting for 22% and 33%.

4.5. Ablation experiment

An ablation experiment on the model structure and auxiliary features was conducted to assess the distinct contributions of each component on our

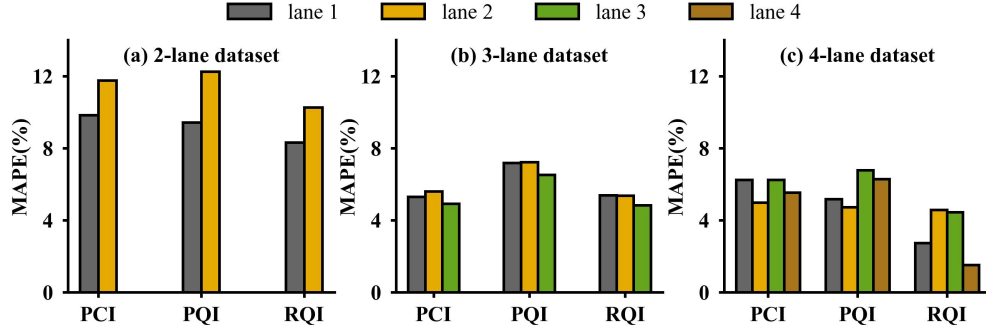


Figure 4: The lane-level MAPE of our model

4-lane dataset. Regarding the model structure, three different test models were implemented. As for the auxiliary features, each feature was removed individually to assess its impact.

There are test models' introductions. In test model 1, the LSTM-based shared layer is removed, so the pavement performance time series are sent directly to each task-specific head. The shared layer typically extracts common features from the input data, offering a universally applicable prediction outcome for all lanes. Furthermore, these layers incorporate a regularization effect that helps prevent over-fitting to any single task. In test model 2, the model eliminates the multiple task-specific heads. Instead, the output from the LSTM-based shared layer is transformed into a 2-dimensional format and then horizontally concatenated with auxiliary features. The presence of task-specific heads, each focusing on the prediction of a specific lane, can enhance predictive performance by concentrating on the relevant features and patterns most indicative of the outcomes for each lane. This specialization improves the accuracy and reliability of the predictions. In test model 3, the horizontal concatenation process is removed. The original model integrates auxiliary features that enhance its ability to represent input data. This integration is conducive to capturing the varied impacts on pavement performance deterioration more comprehensively, including factors such as traffic load and pavement material. It enables the model to detect more subtle and complex patterns. Moreover, feature integration provides increased regularization, which helps to mitigate the risk of over-fitting.

Our model and test models are used to predict PCI, PQI, and RQI, and the MAPE results are shown in Figure 8(a). The results indicate that all the

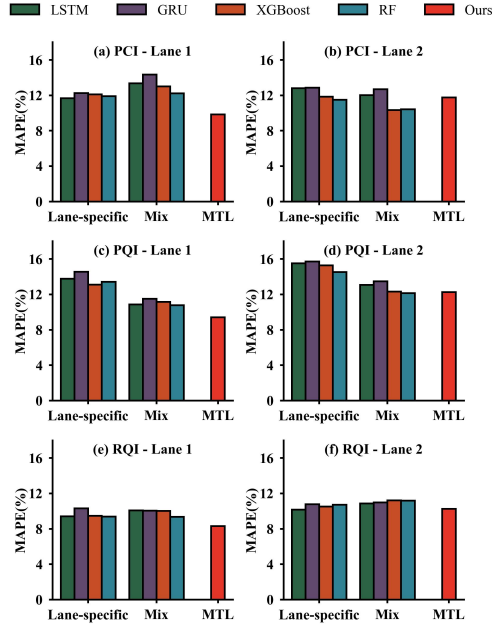


Figure 5: The lane-level MAPE on the 2-lane dataset

components contribute positively to enhancing the accuracy of the predictions. The LSTM-based shared layer is of the most significant importance to our model. When this shared layer is removed, the MAPE increases by 1.631%, 1.611%, and 1.806% when predicting PCI, PQI, and RQI, respectively. To validate the impact of every auxiliary feature on the model’s predictive performance, each auxiliary feature was removed individually, and the MAPE results are shown in Figure 8(b). The results indicate that all the utilized auxiliary features contribute positively to enhancing the accuracy of the predictions. Also, there is not one feature that will greatly improve prediction accuracy. The reduction of MAPE ranges from 0.227% to 0.547% when predicting PCI, 0.300% to 0.697% when predicting PQI, and 0.245% to 0.663%.

5. CONCLUSION

Lane-level performance predictions offer more granular information for developing subsequent maintenance strategies and creating maintenance plans compared to segment-level predictions. The paper proposed a multi-task

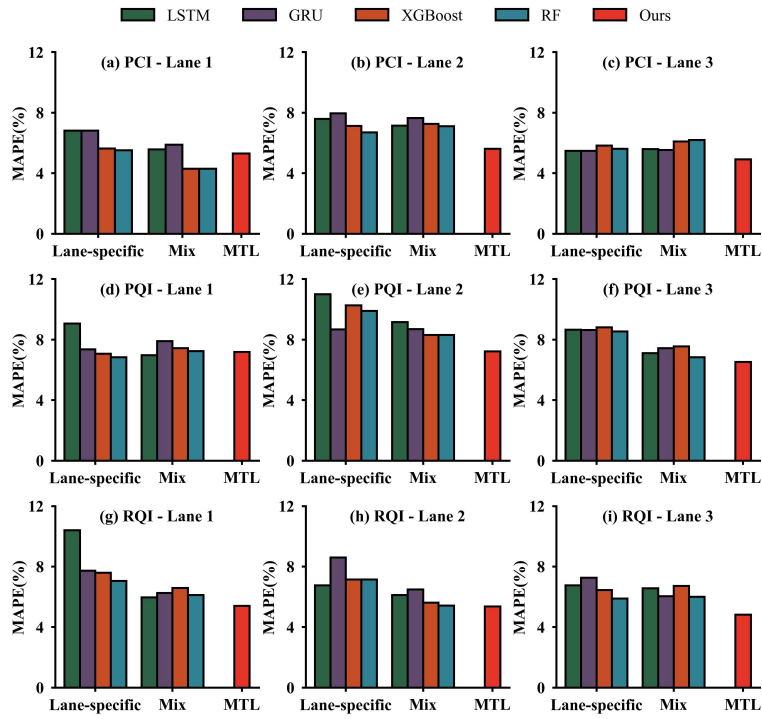


Figure 6: The lane-level MAPE on the 3-lane dataset

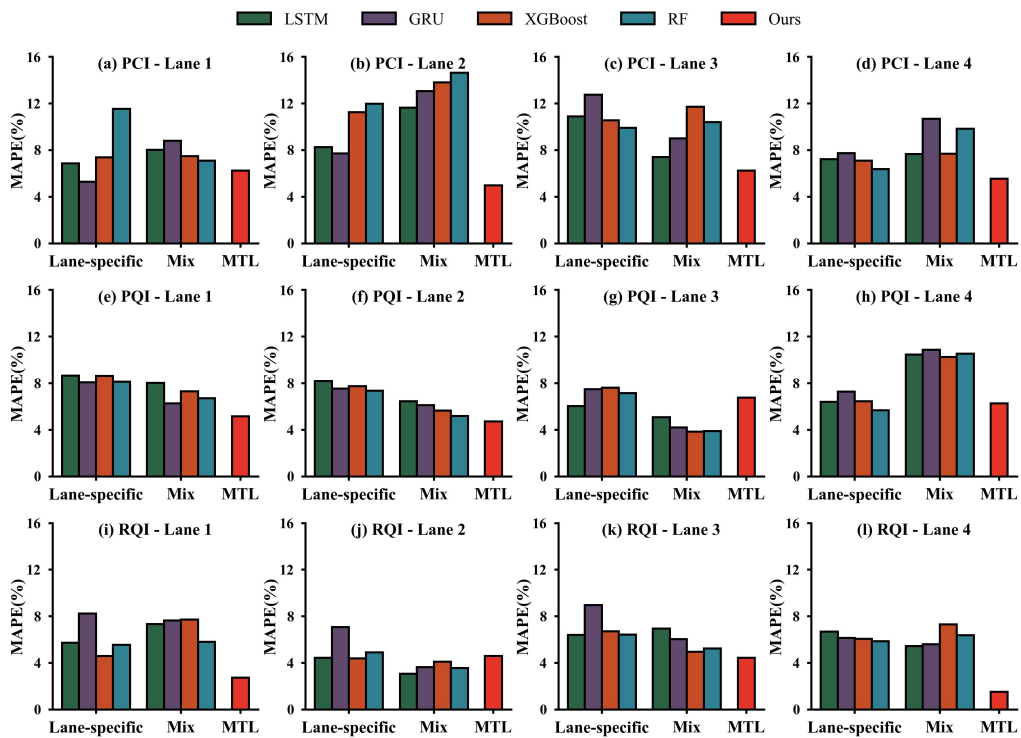


Figure 7: The lane-level MAPE on the 4-lane dataset

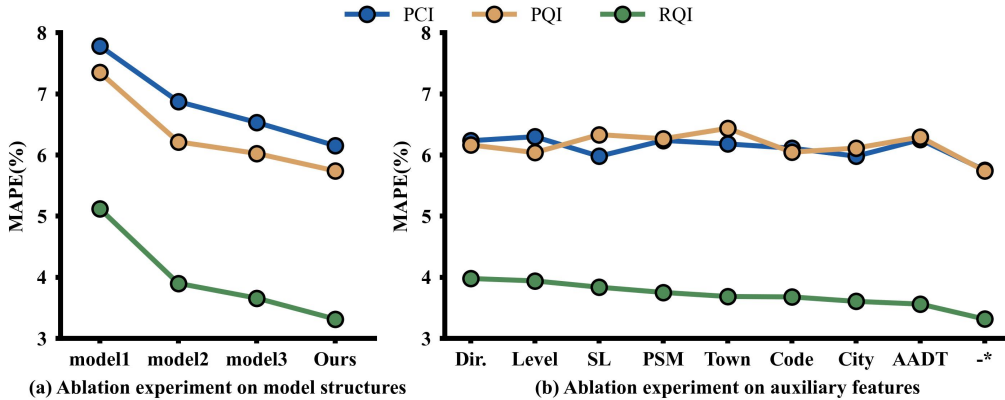


Figure 8: The MAPE of ablation experiments
 Note: - means there is no feature removed.

deep learning approach, accounting for the similarities and differences in pavement performance time series and auxiliary features of different lanes, for lane-level pavement performance prediction based on segment-level pavement inspection data. It has undergone rigorous validation and ablation experiments using segment-level pavement inspection data from Zhengzhou, Jiaozuo, and Luoyang in Henan Province, China. The principal conclusions are presented below.

(1) Our model performs better in predicting PCI, PQI, and RQI based on three distinct datasets. It illustrates the efficacy of multitask-learning based model in leveraging related tasks to improve overall and task prediction precision in pavement performance prediction.

(2) Increasing the number of lanes predicted simultaneously can improve the prediction accuracy of the overall and each task and achieve higher performance improvement compared to other models.

In addition, there are still two issues deserving in-depth discussions. First, the spatial relationship of the prediction units should be further explored during the prediction. Since the prediction units of adjacent positions usually have similar and correlated performance. Second, very few prediction units may happen sharp drops in pavement performance, which results in worse prediction accuracy.

References

- [1] Abdualmtalab Abdualaziz Ali, Usama Heneash, Amgad Hussein, and Shahbaz Khan. Application of artificial neural network technique for prediction of pavement roughness as a performance indicator. *Journal of King Saud University - Engineering Sciences*, 36(2):128–139, 2024.
- [2] Yuanjiao Hu, Zhaoyun Sun, Lili Pei, Wei Li, and Yingying Li. Evaluation of pavement surface roughness performance under multi-features conditions based on optimized random forest. In *2021 Ninth International Conference on Advanced Cloud and Big Data (CBD)*, pages 133–138, 2022.
- [3] Ming Wu, Duanyi Wang, and Chaoxu Lei. Research on asphalt pavement performance prediction model. *Guangdong Highway Communications*, pages 5–9, 2009.
- [4] Liping Cao, Lingwen Li, Chen Yang, Bingtao Zhang, and Zejiao Dong. Performance prediction of expressway pavement in high maintenance level areas based on cosine deterioration equation: A case study of zhejiang province in china. *Journal of Road Engineering*, 2(3):267–278, 2022.
- [5] Amnon Ravina Arieh Sidess and Eyal Oged. A model for predicting the deterioration of the international roughness index. *International Journal of Pavement Engineering*, 23(5):1393–1403, 2022.
- [6] Hainian Wang. Calibration of rutting prediction model in mepdg based on mathematical statistics method. *Journal of Chang’an University*, 2013.
- [7] Shi Dong, Peiwen Hao, Minjiang Zhang, and Qicheng Xu. Method for asphalt pavement deterioration forecasting based on panel-data markov. *Journal of Beijing University of Technology*, 42(11):1703–1712, 2016.
- [8] Xiaolan Wang. Prediction of pavement performance based on the grey markov model for small sample sizes. *Transport Business China*, 33(11):25–27, 2023.
- [9] Khaled A. Abaza. Optimal novel approach for estimating the pavement transition probabilities used in markovian prediction models. *International Journal of Pavement Engineering*, 23(8):2809–2820, 2022.

- [10] Samiulhaq Wasiq and Amir Golroo. Probabilistic pavement performance modeling using hybrid markov chain: A case study in afghanistan. *Case Studies in Construction Materials*, 20:e03023, 2024.
- [11] Xuancang Wang, Jing Zhao, Qiqi Li, Naren Fang, Peicheng Wang, Longting Ding, and Shanqiang Li. A hybrid model for prediction in asphalt pavement performance based on support vector machine and grey relation analysis. *Journal of Advanced Transportation*, 2020.
- [12] Manzhe Xiao, Rong Luo, Yu Chen, and Xinmin Ge. Prediction model of asphalt pavement functional and structural performance using pso-bpnn algorithm. *Construction and Building Materials*, 407:133534, 2023.
- [13] Rui Tao, Pengfei Ding, Rui Peng, and Jiangang Qiao. Prediction of asphalt pavement performance based on depso-bp neural network. *Canadian Journal of Civil Engineering*, 50(8):709–720, 2023.
- [14] Abdualmtalab Abdualaziz Ali, Usama Heneash, Amgad Hussein, and Shahbaz Khan. Application of artificial neural network technique for prediction of pavement roughness as a performance indicator. *Journal of King Saud University - Engineering Sciences*, 36(2):128–139, 2024.
- [15] Wenyuan Cai, Andi Song, Yuchuan Du, Chenglong Liu, Difei Wu, and Feng Li. Fine-grained pavement performance prediction based on causal-temporal graph convolution networks. *IEEE Transactions on Intelligent Transportation Systems*, 25(5):4606–4619, 2024.
- [16] Alexander W. Bukharin, Zhongyu Yang, and Yichang James Tsai. Five-year project-level statewide pavement performance forecasting using a two-stage machine learning approach based on long short-term memory. *Transportation Research Record*, 2675:280 – 290, 2021.
- [17] Jeremy Gregory Fengdi Guo, Xingang Zhao and Randolph Kirchain. A weighted multi-output neural network model for the prediction of rigid pavement deterioration. *International Journal of Pavement Engineering*, 23(8):2631–2643, 2022.